CONTROL SYSTEMS LABORATORY

SAMPLING DISTRIBUTION OF THE AUTOCORREIATION AND POWER SPECTRUM FUNCTIONS

DA-36-039-SC-56695
D/A Sub-Task 3-99-06-111

UNIVERSITY OF ILLINOIS · URBANA · ILLINOIS

The research reported in this document was made possible by support extended to the University of Illinois, Control Systems Laboratory, jointly by the Department of the Army (Signal Corps and Ordnance Corps), Department of the Navy (Office of Naval Research), and the Department of the Air Force (Office of Scientific Research, Air Research and Development Command), under Signal Corps Contract DA-36-039-SC-56695, D/A Sub-Task 3-99-06-111.

Report Number R-78

SAMPLING DISTRIBUTION OF THE AUTOCORRELATION AND POWER SPECTRUM FUNCTIONS

Prepared by:

Leroy Augenstine

January 1957

CONTROL SYSTEMS LABORATORY
UNIVERSITY OF ILLINOIS
URBANA, ILLINOIS
Contract DA-36-039-SC-56695

Numbered Pages: 35

SAMPLING DISTRIBUTION OF THE AUTOCORRELATION AND POWER SPECTRUM FUNCTIONS

Leroy Augenstine

It has been reported previously,[1,2] that while performing simple tasks of information processing a human does not operate in a smooth or continuous fashion, but rather his actions are quantized. This was inferred from the fact that the distribution of response times was "lumpy" rather than smooth. Not only were the distributions multimodal but the modes, which were the most probable reporting times, occured at regular intervals, i.e., the response times exhibited periodic behaviour. A number of analytical methods have been used to search for these periodicities, of which the most promising are those described by Seiwell[3] and Tukey.[4,5]

The autocorrelation function (AC) in the form used by Seiwell is given by

$$(1)\quad R_k = \frac{\overline{x_i \cdot x_{i+k}} - \overline{x_i}\cdot\overline{x_{i+k}}}{\sigma_i \cdot \sigma_{i+k}} \qquad \begin{array}{l} k = 0, 1, 2, \ldots m \\ i = 1, 2, 3, \ldots N-k \end{array}$$

where

$\underline{R_k}$ is the $\underline{k}$th value of the AC function.

$\underline{x_i}$ is the value of the $\underline{i}$th interval of the histogram; i.e., x_i is the frequency with which response times of $\underline{i}$ intervals (of 10 msec.) longer than the shortest response are observed.

$\overline{x_i \cdot x_{i+k}}$ is the average of the (N-k) products of the form $x_i \cdot x_{i+k}$ for $0 \leq i \leq N-k$.

$\overline{x_i}$ is the mean of the x_i's for $0 \leq i \leq N-k$.

$\overline{x_{i+k}}$ is the mean of the x_i's for $k \leq i \leq N$.

$\underline{\sigma_i}$ is the standard deviation of the x_i's for $0 \leq i \leq N-k$.

$\underline{\sigma_{i+k}}$ is the standard deviation of the x_i's for $k \leq i \leq N$.

The cosine series representation of the Fourier transform of the AC function in eq. 1 was used in the spectral density function; it is similar to the correlation expression suggested by Tukey. This form was chosen since it contains terms to help correct for the non-constant average amplitude existing in the histograms. The description of the operations involved is:

$$(2)\quad U_p = \sum_{k=o}^{m} b_k R_k \cos kp\pi/m; \quad p = 0, 1, 2, \ldots m$$

$$(2a)\quad b_k = 0.52 + 0.46 \cos k\pi/m$$

where U_p is the pth coefficient of the Fourier cosine series representation of the autocorrellogram, and

b_k is a smoothing function suggested by Tukey[6,7] to make peaks in U_p more pronounced.

Some of the characteristics of these two methods are described in the appendix.

The power spectrum (PS) method will be emphasized in this report; it seems to be the preferable method since it involves a further reduction of the data obtained from the AC. However, the PS analysis, since it involves a Fourier transformation, is designed to give optimum results with periodic data which have a sinusoidal wave form. But, it would be a little surprising if humans exhibited sinusoidal periodicities. Further, it is necessary to deal with fairly small data samples to avoid fatigue effects, which means that the wave form may not be readily discernible from a given set of data.

Thus it was felt that a study should be made of the sampling distributions of the AC and PS methods. A complete study would involve determining the effect of the wave form and the position and height of maxima in the time series on the distribution of the AC and PS. Work bearing on these

problems has been reported by Tukey[4] and Ross[8]. However, it is not clear if these methods apply fully to data with the properties mentioned above. As a result we have attempted a limited study of the sampling distributions of the AC and PS methods for one wave form (Gaussian) and situations comparable to those encountered in our experiments. Rather than making a thorough investigation of the behavior of these functions we have concentrated on synthesizing data according to mathematical models which it was hoped simulated the behavior of our subjects. These synthesized data were analyzed according to the AC and PS methods. From comparisons between the results of these analyses and those obtained from human data it was possible to modify the mathematical models and determine the range of parameters from which comparable values resulted. By such an iterative procedure reasonable agreement was eventually obtained between the results from synthesized and human data. The data which have been analyzed have not only helped to improve the model but have yielded results which indicate the efficiency and limitations of such methods for analyzing this type of data. Consequently, these results and procedures are worthy of presentation.

It was found that the composition of the PS depended not only on the periodicities present but also the general shape of the time series. In fact in some situations the peak in the PS corresponding to the main periodicity was overshadowed by other peaks resulting from the general shape of the time series. A more diffuse wave form can be detected in the PS than in the AC.

From the results, it seems reasonably certain that a fairly strong quantization of 100 msec. is associated with simple information

processing in man. Also, there is a suggestion that the fundamental quantum may be 33.3 msec. in duration, with three of them grouped together to give the strong 100 msec. periodicity.

METHODS

The data have all been synthesized by the use of Monte Carlo techniques* In our basic mathematical model of the human we ascribed a reaction time, T, as being the sum of the following components (see eq. 2 of R-75):

$$(3)\quad T = (t_o+\gamma_o)+\beta(t_i+\gamma_i)+\alpha(t_p+\gamma_p)$$

where t_o is the time necessary for accommodation, to decide upon the operating procedure which is best for the given situation and to generate a response; t_i is the duration of the quantization associated with data input; t_p is the duration of the quantization associated with the unit acts by which information is processed; the γ's represent the distributions associated with the various t's (i.e., the disperseness of the distributions of the γ's represents the sloppiness of humans in performing the data processing); and β and α are integers which are respectively the number of input and processing cycles required to complete the task. The α, β and γ's are thus seen to be random variables selected from their respective distributions; these were the random variables which were generated by Monte Carlo methods.

A given set of data was synthesized by specifying the durations of the t's and the distributions and ranges associated with the various random variables. A particular response time, T, (in units of 10 msec.) was

---

* Synthesis and analysis of the data were performed on ILLIAC, the electronic digital computer at the University of Illinois.

formed by generating an α, β, γ_i, γ_o and γ_p. The number of T's generated for a given set of synthetic data was specified in the problem and corresponded to a sample size, s, obtained from our subjects. The s response times were then tabulated into a histogram of response time frequencies and analyzed exactly the same as the human data* i.e., the number of times 420 msec., 430 msec., 440 msec., ...570 msec. ....etc. occurred was tallied.

Examination of some of the preliminary human data indicated that the α's and β's had a somewhat rectangular distribution, the γ's probably a Gaussian distribution and there was very often one outstanding period. Thus much of the synthetic data involves a single 100 msec. quantum and distributions for α, β and γ mentioned above. However, it was necessary to modify some of the parameters before a reasonable agreement between synthetic and human results was obtained. These modifications included the substitution of a distribution very similar to a Poisson in place of the rectangular ones and the assumption that although 100 msec. is the most pronounced periodicity it is actually composed of a group of three quanta of 33 msec.

---

* It should be pointed out that such a histogram is not a time series obtained in the usual manner. However, its relation to the usual time-probability curve can be seen from the following hypothetical situation. Suppose a very large number of equivalent subjects began the same task simultaneously, and the number responding in each time interval was observed. A frequency-time interval plot of the data would give the usual time series, and with a complete representation of the wave form of any periodicities present. What we have done is to collect only a small sample of data from one subject (or generate only a limited sample size). This corresponds to collecting data from a few identical subjects who began their tasks sequentially rather than simultaneously. Such a procedure, of course, will only generate incomplete portions of the wave form.

RESULTS*

MI. In the first model (MI) a single periodicity was used (β was set equal to 0). α was assigned a rectangular distribution with values from 1-30 and γ_p and γ_o were assigned Gaussian distributions with standard deviations, σ_p and σ_o.** The data in fig. 1 indicate the effect of varying σ_o when $\sigma_p = o$, $t_p = 100$ msec., α had a range of 1-30 and 150 response times were generated. The range of 3 sec. (30 periods of 100 msec.) corresponds to the usual range of the human reaction times. Of particular interest is the increase in what are spurious peaks (i.e., peaks not corresponding to the periodicity of 100 msec.) as σ_o increases in size. These occur because the plots are not of U_p but of U_p/U_{max}, and the more diffuse the wave form of the periodicity the lesser the maximum spectral density value; thus, small background clutter will increase with respect to U_{max} until it finally assumes an apparent importance. In this manner it will appear that new pseudo-periodicities are occurring. Thus, the normalization which is quite convenient for computer operation can cause some trouble in the analysis, particularly if σ_o approaches 1/3 to 1/2 of the predominant periodicity. However, for $\sigma_o \leq 1/4\ t_p$ little trouble is encountered.

---

* It is necessary to bear in mind that the PS abscissa (p) is a frequency scale and not a linear time scale. The cos $kp\pi/m$ term becomes maximum $p/2$ times in the interval $0 \leq k \leq m$. Thus, the maxima of cos $kp\pi/m$ occur at integral multiples of $2m/p$. If m=100, a periodicity of 100 msec. would be represented by a peak at p=20 (2000/20=100) and a peak at p=60 would indicate a period of 33.3 msec. (2000/60=33.3).

** t_o was usually set equal to 400 msec.; however, this is unimportant since it merely shifts the origin of the time series but does not affect the AC or PS.

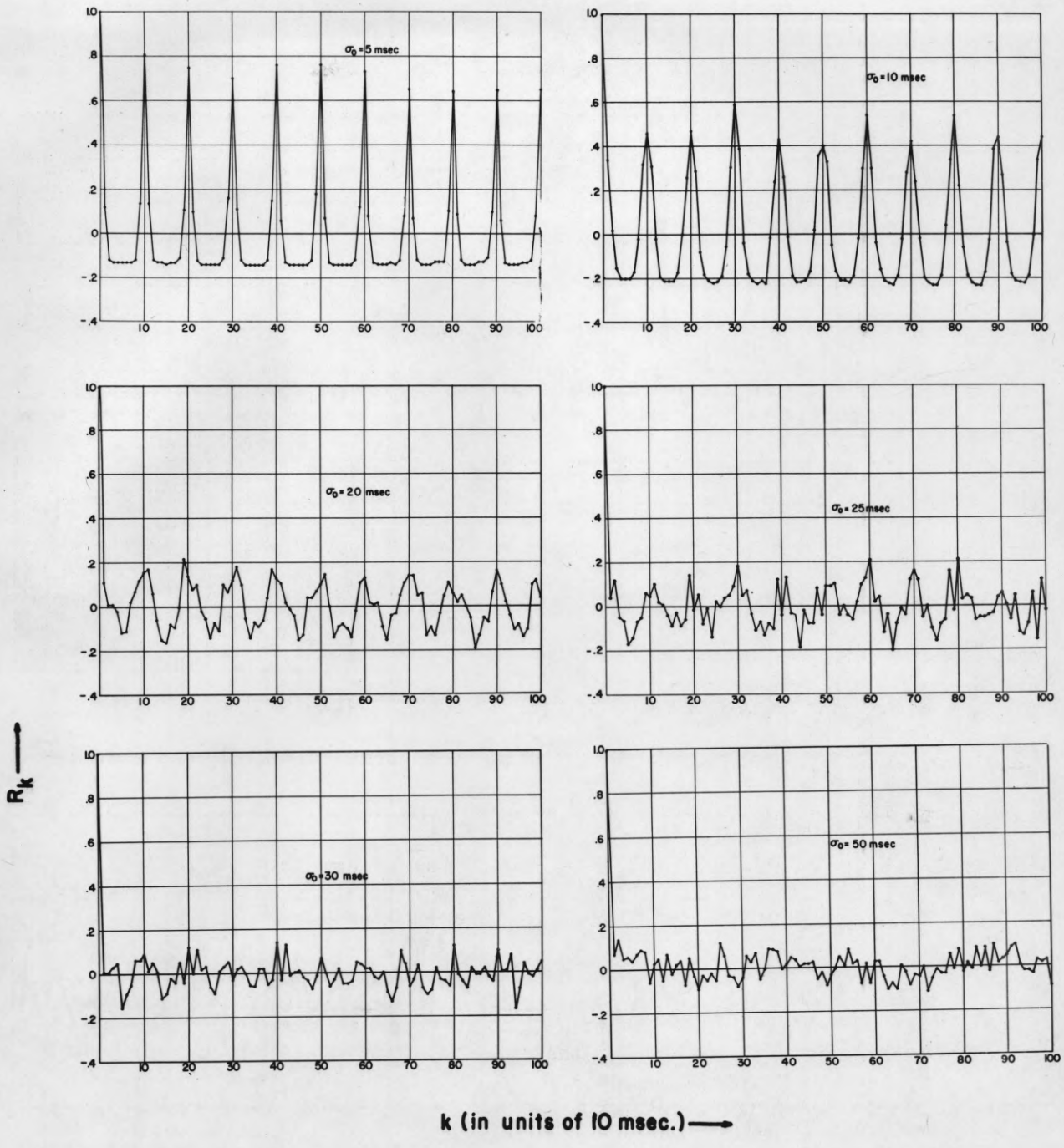

FIG. 1A THE EFFECT ON THE AUTOCORRELOGRAMS OF VARYING σ_0 WHEN $\sigma_p = 0$; t_p = 100 MSEC., $1 \leq \alpha \leq 30$, β=0 AND S=150. DATA WERE GENERATED ACCORDING TO MODEL MI APPLIED TO EQUATION (1):

$$T=(t_0+\Delta_0)+\beta(t_i+\Delta_i)+\alpha(t_p+\Delta_p)$$

WHERE THE σ's ARE THE STANDARD DEVIATIONS OF THE GAUSSIAN DISTRIBUTIONS (Δ's) ASSOCIATED WITH THE VARIOUS t's. (THE SUBSCRIPT i REFERS TO THE INPUT OF DATA, p TO DATA PROCESSING AND $_o$ TO THE DETERMINATION OF AN OPERATING PROCEDURE AND A RESPONSE.) HENCEFORTH, t_0 WAS SET EQUAL TO 400 MSEC. BUT CAN BE DISREGARDED SINCE IT PRODUCES NO EFFECT ON EITHER THE AC OR PS. (SEE TEXT)

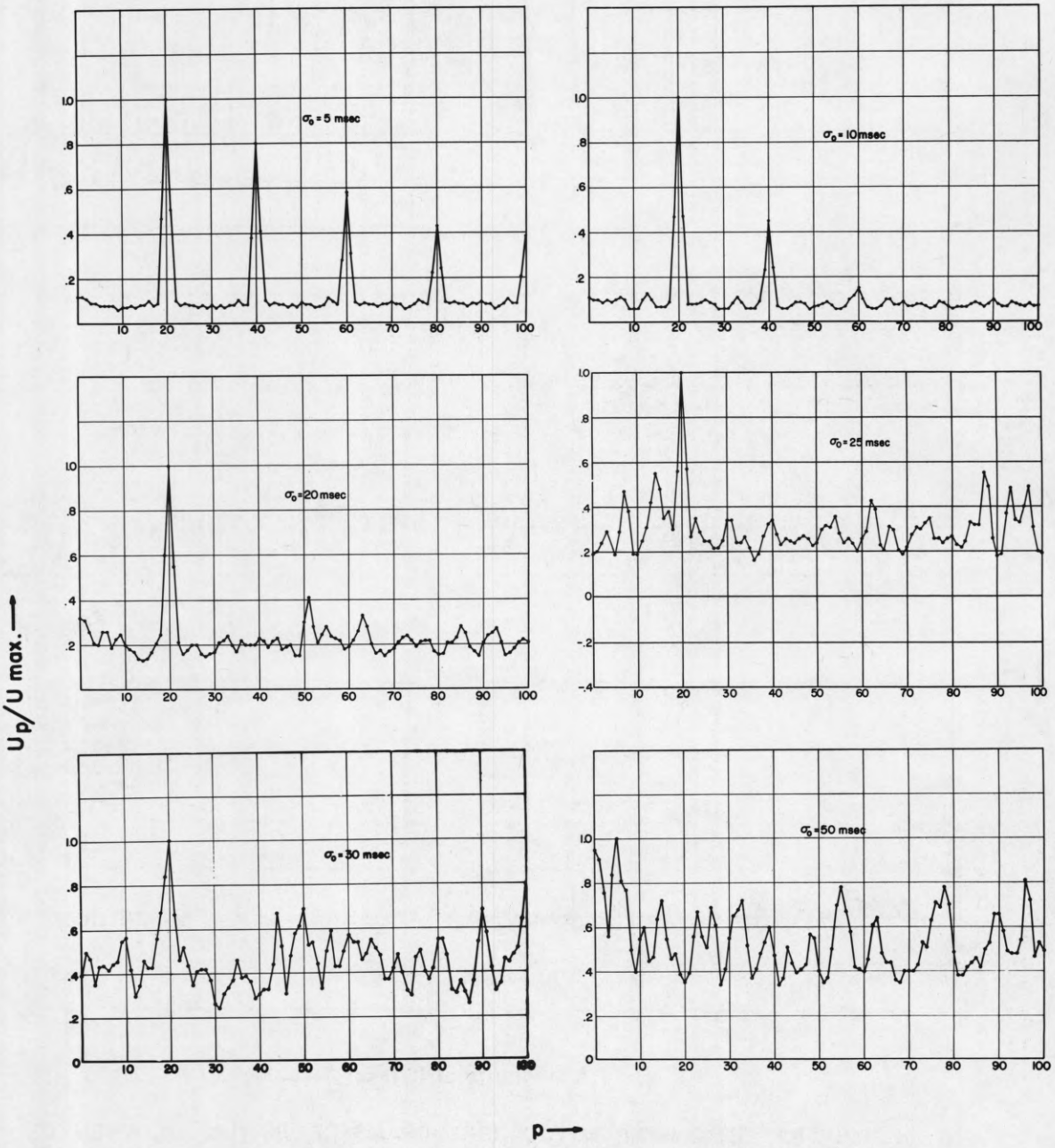

FIG. IB THE EFFECT ON THE POWER SPECTRA OF VARYING σ_0 WHEN $\sigma_p = 0$. OTHER FACTORS ARE THE SAME AS IN FIG. IA.

Although the detection of the 100 msec. period depends critically upon σ_o, it can be seen in fig. 2 that the detection is relatively insensitive to sample size - at least for an average data density of greater than 2 observations per period.

The data shown in fig. 3 indicate the effect of γ_p alone. From these results it was possible to set limits on the values of the parameters which when inserted into eq. 3, would give results compatible with the human data (R-75). σ_p should be less than 6 msec. and σ_o should lie between 10 and 35 msec. The results of various combinations of the two parameters are shown in figs. 4 and 5.

It can be seen in figs. 1-5 that as σ increases the 100 msec. periodicity becomes obscured quicker in the AC than in the PS. However, the PS has the unfortunate property, mentioned previously, that its background increases as σ increases. It can also be seen that the effect of σ_p is roughly comparable to a 5-7 times larger increase in σ_o for the factors we have investigated. Actually σ_o and σ_p are not equivalent since σ_p causes the modes associated with large α's to be more disperse than those associated with small α's but not to shift the locus of the mode along the time scale; whereas, the effect of σ_o is independent of α. An investigation of the human data indicated that there was not a marked difference in the disperseness of early modes as contrasted to late modes so that it appears justified to assume that the variability is largely due to γ_o. Henceforth, σ_p and σ_i were set to zero and γ_o made large enough to take care of all of the variance.

Some of our early human data was collected under conditions in which the accuracy of the response times was $\pm$ 10 msec., which was

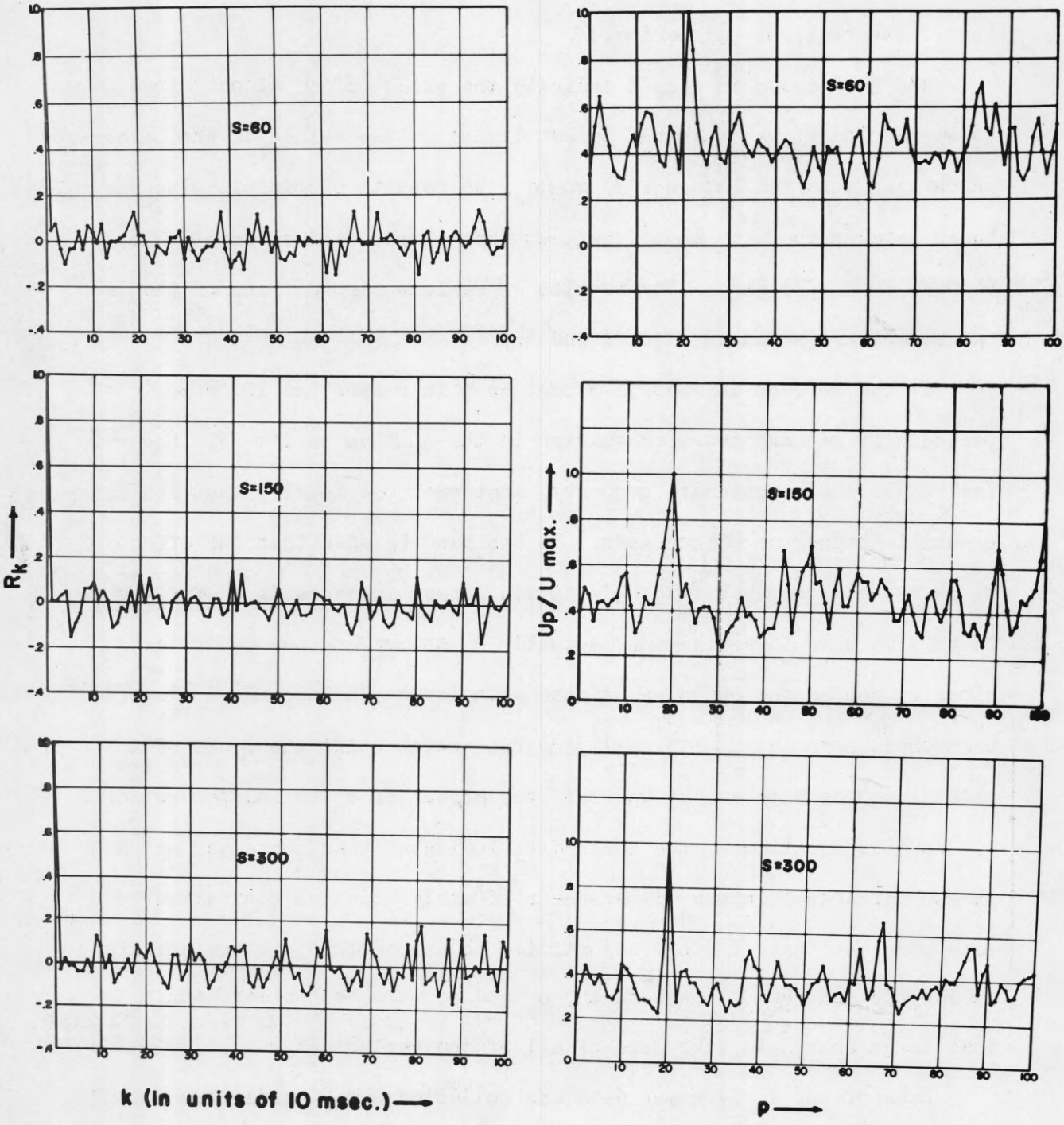

FIG. 2 THE EFFECT OF THE SAMPLE SIZE ON THE AC AND PS WHEN t_p = 100 MSEC., σ_0 = 30 MSEC., σ_p = 0, $1 \leq \alpha \leq 30$, β=0 AND USING MI. WITH THESE FACTORS EQUATION 1 HAD THE FORM:

$$T(\text{MSEC.}) = 400 + \Delta_0 + 100\alpha$$

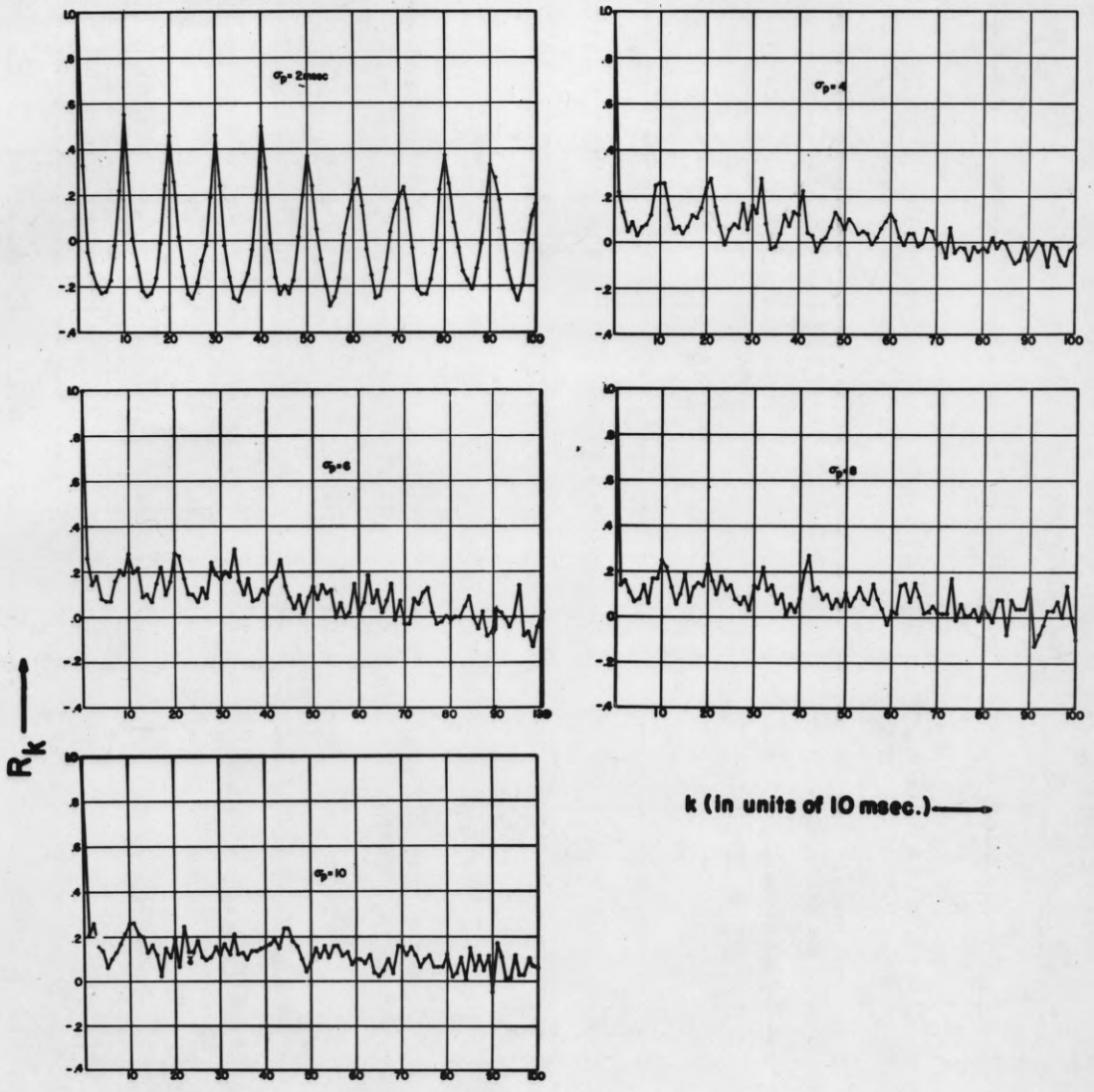

FIG. 3A THE EFFECT ON THE AC OF VARYING σ_p WHEN $\sigma_0 = 0$, t_p=100 MSEC., $1 \leq \alpha \leq 30$, β=0, S=300. DATA WERE GENERATED USING MI. THESE FACTORS GAVE EQUATION (1) THE FORM:

$$T(\text{MSEC}) = 400 + \alpha(100 + \Delta_p).$$

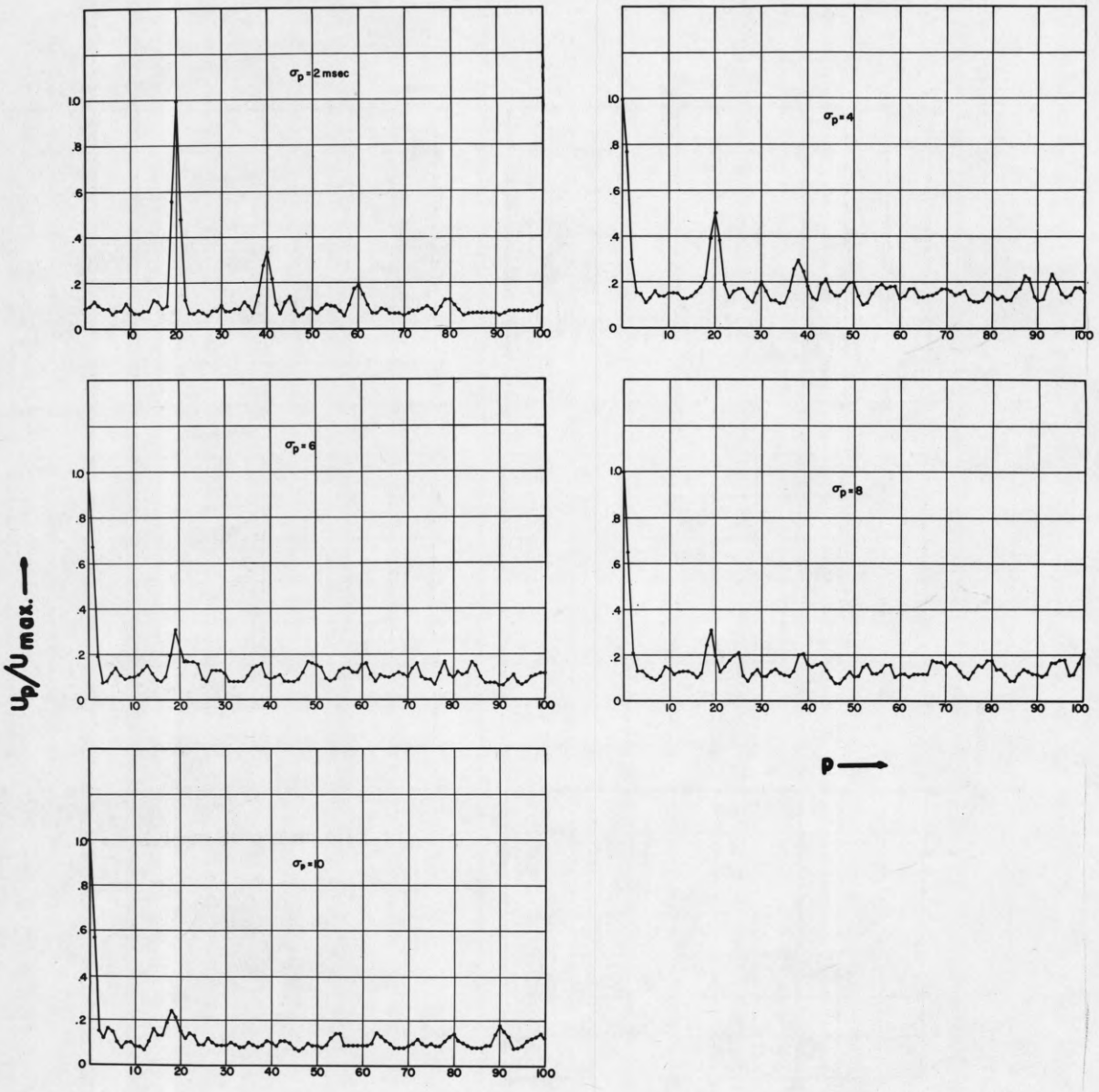

FIG. 3B THE EFFECT ON THE PS OF VARYING σ_p WHEN $\sigma_0 = 0$. OTHER FACTORS ARE THE SAME AS IN FIG. 3A.

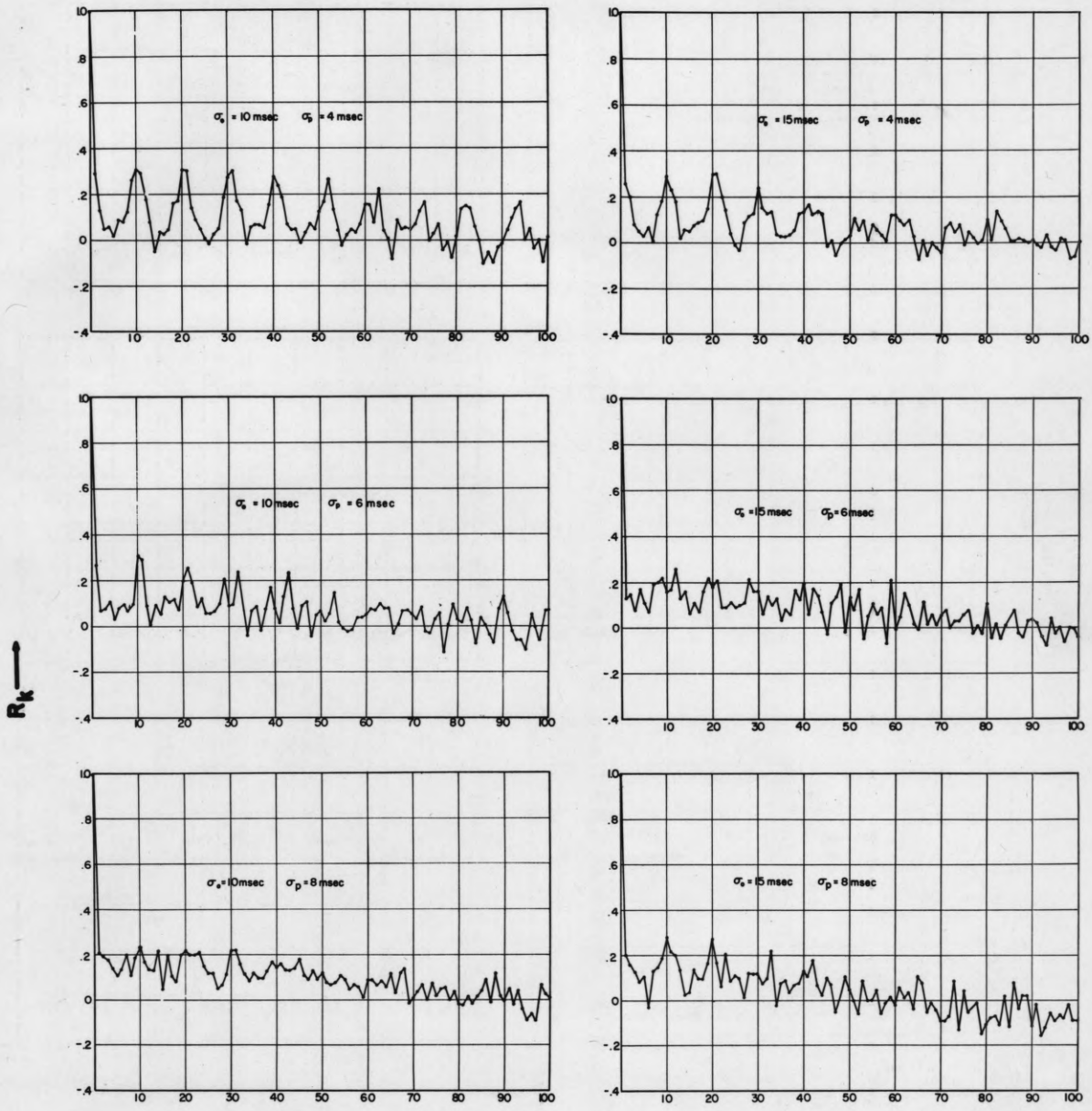

FIG. 4A THE EFFECT ON THE AC OF VARYING BOTH σ_0 AND σ_p WHEN t_p = 100 MSEC., $1 \leq \alpha \leq 25$, $\beta = 0$, S = 300 AND USING MI. THESE FACTORS GAVE EQUATION (1) THE FORM:

$$T(\text{MSEC}) = 400 + \Delta_0 + \alpha(100 + \Delta_p)$$

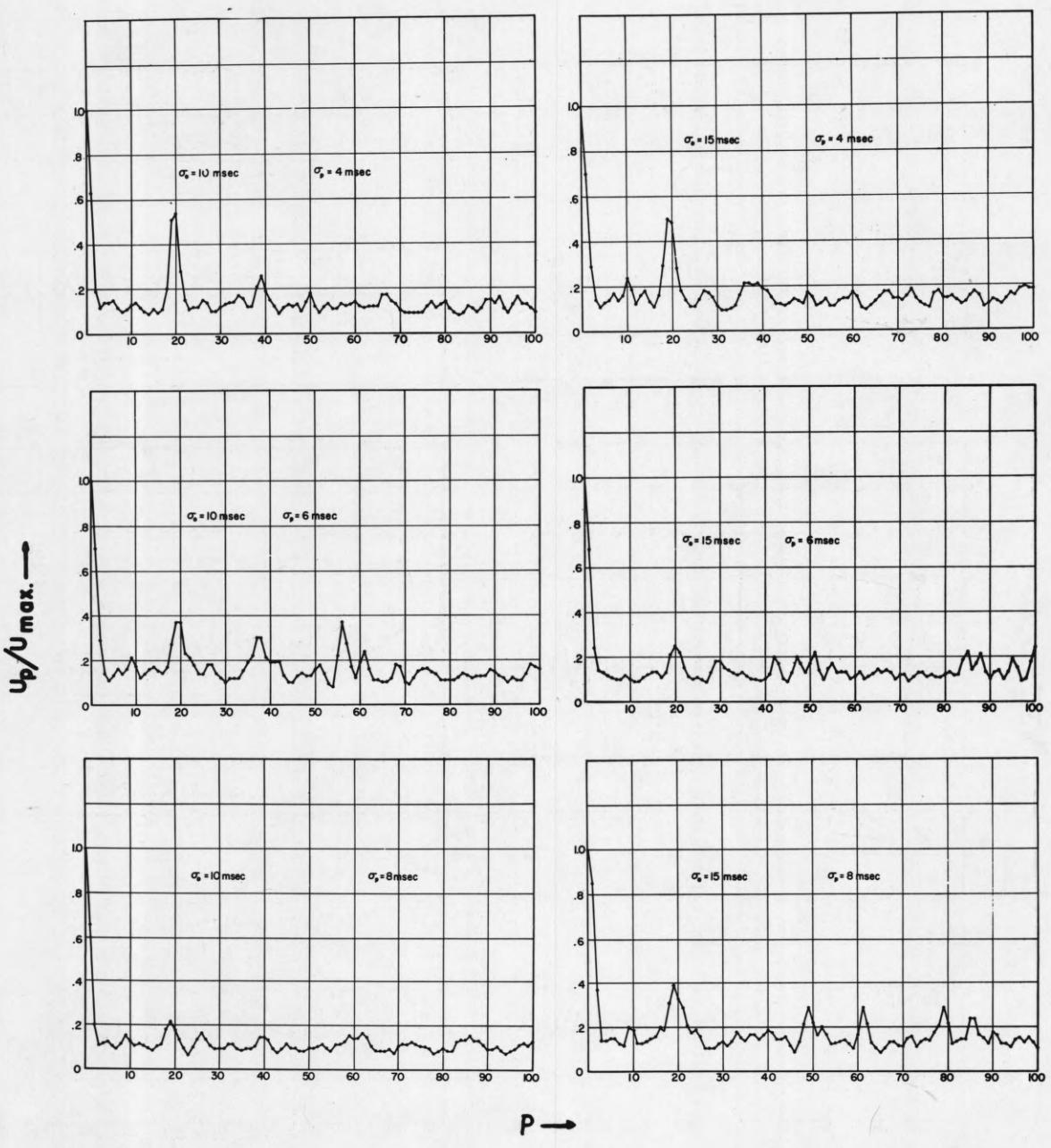

FIG. 4B THE EFFECT ON THE PS OF VARYING BOTH σ_o AND σ_p. OTHER FACTORS ARE THE SAME AS IN FIG. 4A.

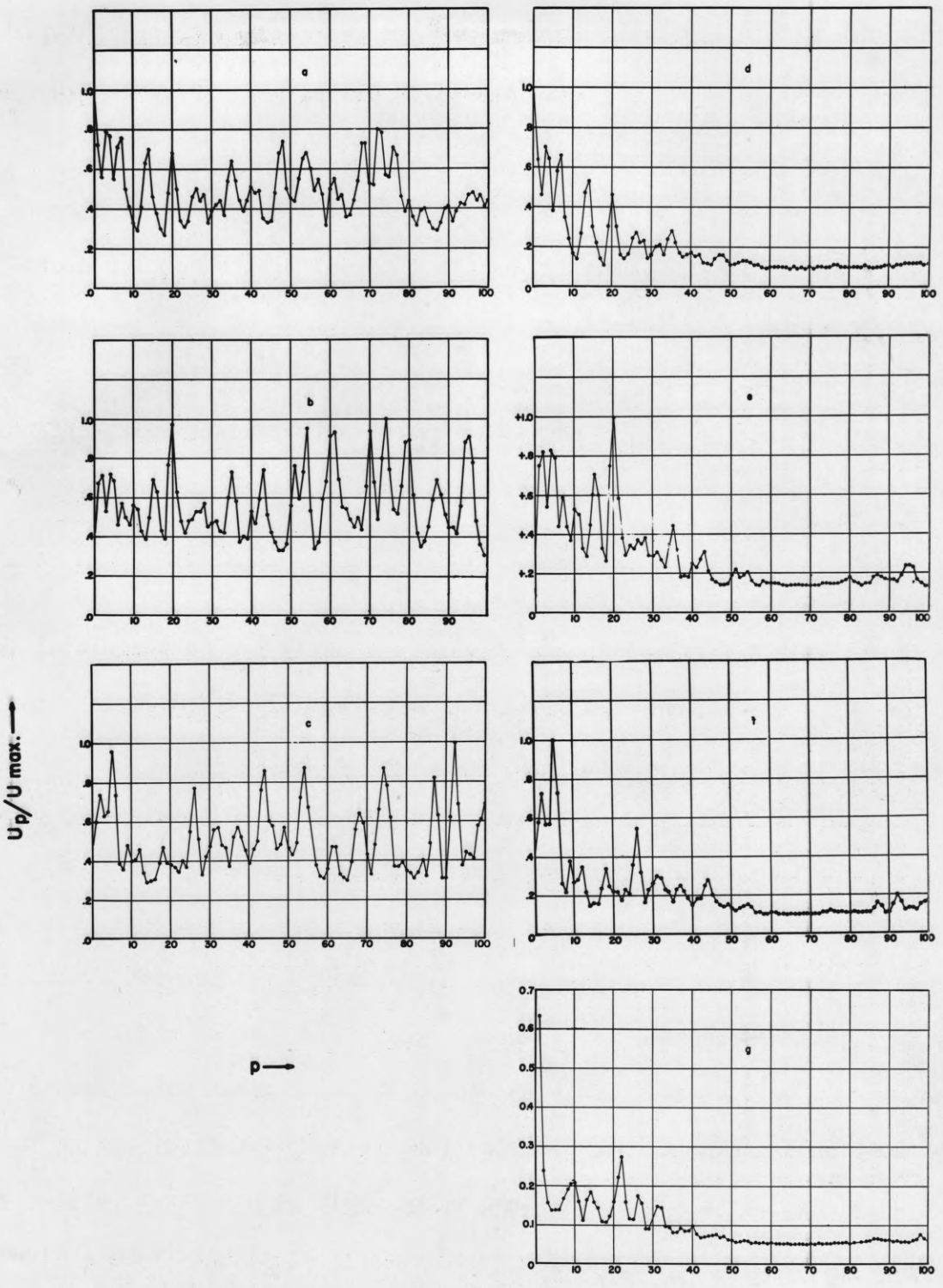

FIG. 5 THE EFFECT ON THE PS OF "SMOOTHING" (EQ.2) THE HISTOGRAM. THE PS ON THE RIGHT ARE FROM "SMOOTHED" HISTOGRAMS, THOSE ON THE LEFT FROM THE CORRESPONDING DATA ASSEMBLED IN UNSMOOTHED HISTOGRAMS. DATA WERE GENERATED ACCORDING TO MODEL MI WITH $1 \le \alpha \le 25$, $\beta = 0$, $s = 300\ (\alpha - f)$ $t_p = 100$ msec., $\sigma_0 = 40$ msec., $\sigma_p = 4$ msec. AND (g) $t_p = 33$ msec., $\sigma_0 = 10$ msec. AND $\sigma_p = 0$ SO THAT EQ.1 HAD THE FORM:

$$T = t_0 + \Delta_0 + \alpha(t_p + \Delta p)$$

equal to the data interval size. In an attempt to avoid complications due to this uncertainty a sliding average process was applied to the initial histograms so as to produce a new "smoothed" histogram.[1] The averaging process applied was:

(4) $X_i = x_{i-1} + x_i + x_{i+1}$ $(i = 1, 2, 3 \ldots N)$

where x_i is the value of the ith interval of the regular histogram and X_i is the value of the ith interval of the "smoothed" histogram.

It can be seen in fig. 5 that this smoothing procedure quite effectively eliminates high frequency components from the PS. If the periodicity being investigated does not fall in the high frequency area, then this smoothing can be of some benefit (however, note plot 5 g).

It was also determined that a PS analysis using b_j, as formulated in relation (2a), was always more effective in detecting periodicities than an analysis in which b_j was omitted, i.e., set equal to 1.

A comparison of a composite power spectrum, fig. 6 (obtained by summing 21 power spectra from six subjects under six experimental conditions) with the results in figs. 1-5 indicated that MI was a poor model. At this stage in the investigation it was suspected that although the largest spectral density value corresponded to 100 msec., that this quantum might be composed of three smaller quanta of about 33 msec. It was further noted that α did not really have a rectangular distribution; rather, the first two or three modes were usually fairly small, then there would be a central portion of the histogram in which the peaks were of roughly equal magnitude followed by a gradual decline in the size of the modes for larger response times. The distributions of the heights of the modes and thus of α look roughly

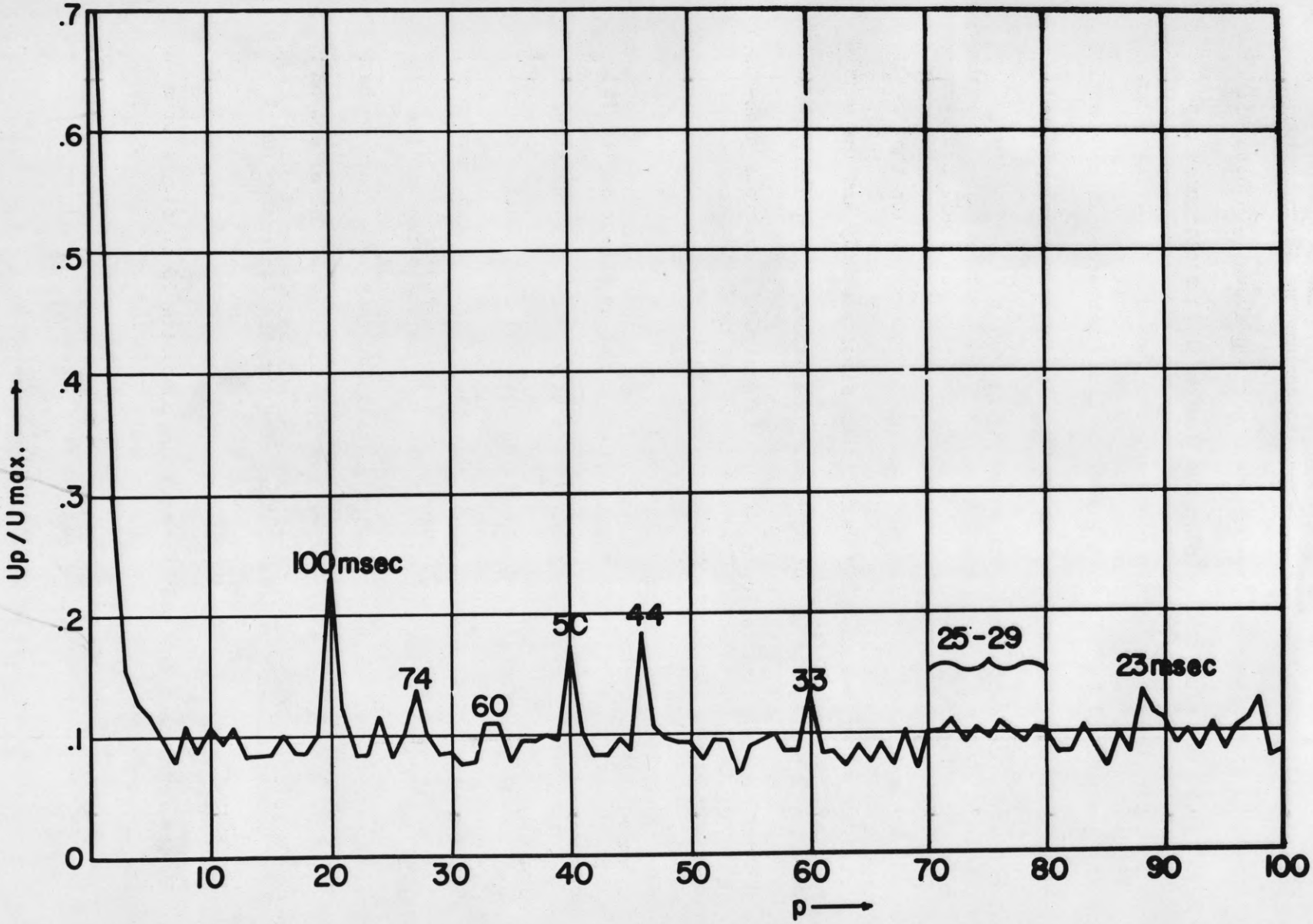

FIG. 6 A COMPOSITE PS CONSTRUCTED BY NORMALIZING THE SUM OF 21 PS OBTAINED FROM 6 SUBJECTS AND UNDER 6 EXPERIMENTAL CONDITIONS.

like Poisson distributions with means ranging from 10-40% of the maximum of α.

MII and MIII. Two attempts were made to change the distribution of α to something approximately like the one described above. In both MII and MIII t_i was set equal to t_p and α and β were given rectangular distributions. In MII the restriction was imposed that β must be less than α for any given T and in MIII that β must be less than one-half α. Results typical of these two models are shown in fig. 7. Neither model yielded results comparable to the composite human PS in fig. 6.

MIV. In the final model t_i and t_p were not only set equal but were combined and designated t_p. This corresponds to the assumption that input and processing occur sequentially rather than simultaneously and the active processes involve the same amount of time. Correspondingly α and β were combined into a single variable, α, which was assigned a discrete probability distribution similar to a Poisson, for each run.

These modifications changed equation 3 to

(5) $T-t_o = \gamma_o + \alpha t_p$ (where t_o, a constant, has no effect on the PS).

Thus, assuming that γ_o has a Gaussian distribution, the only variables are σ_o, t_p, and the general form associated with the distribution of α. The Poisson-like distribution of α was obtained by constructing smoothed "envelopes" through the maxima, i.e., modes, of the histograms of the human response times. When these were normalized, they were found to be quite similar, so that a general envelope could be drawn. The effect on the PS of variations in the distribution of α and the factors σ_o and t_p was tested.

It was found that the best fits to the composite PS in fig. 6 were

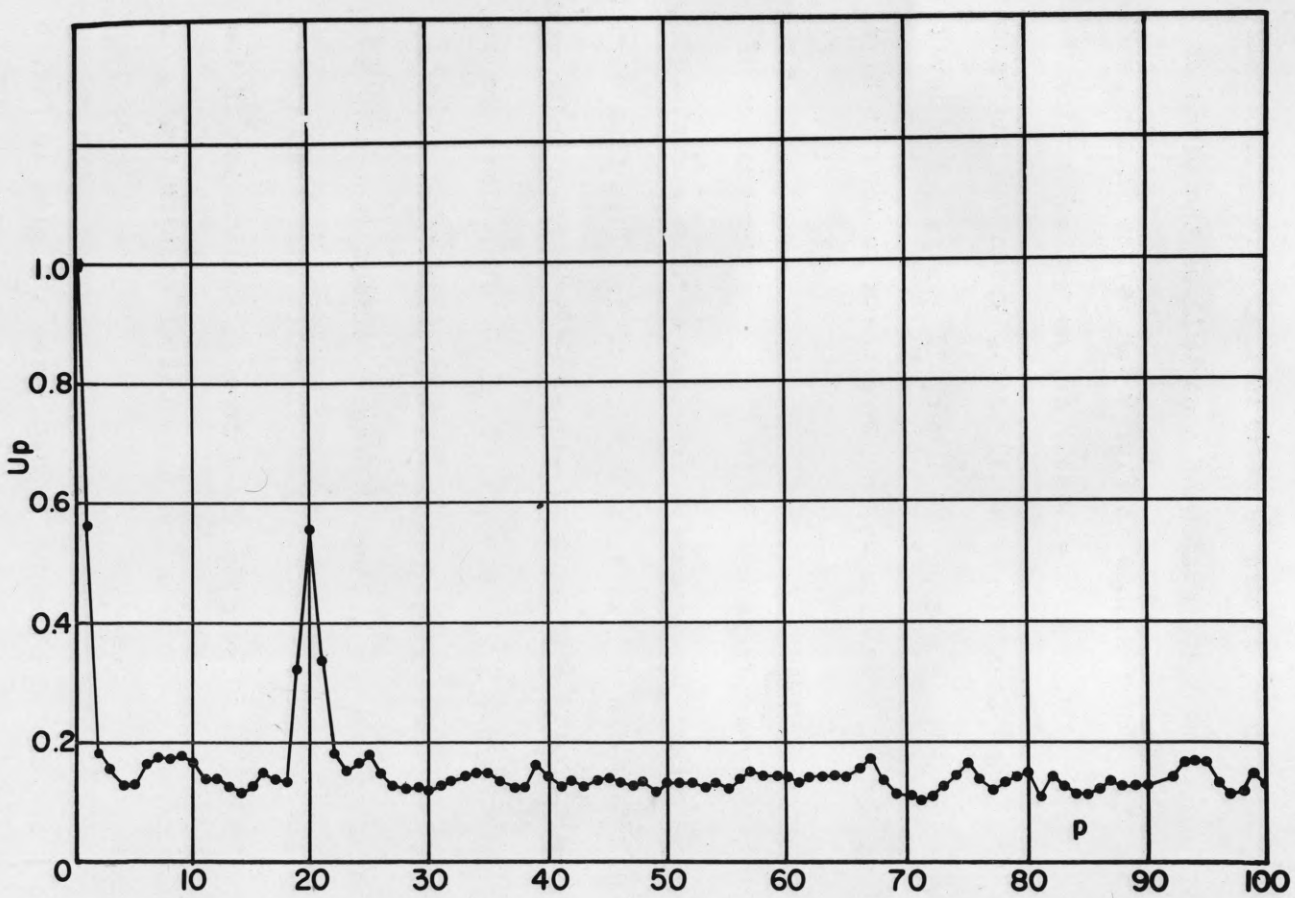

FIG. 7 THE NORMALIZED SUM OF FOUR PS GENERATED ACCORDING TO MII IN WHICH $t_i = t_p = 100$ msec., $\alpha_0 = 20$ msec., $s = 150$, $1 \leq \alpha \leq 25$, WITH THE CONSTRAINT THAT $\beta \leq \alpha$ THESE FACTORS GAVE EQUATION (1) THE FORM:

$$T(\text{msec.}) = 400 + \Delta_0 + 100(\alpha + \beta)$$

obtained if 33 msec. rather than 100 was taken as the duration of t_p. However, portions of the composite PS appeared in the 100 msec. results if a suitable distribution of α was chosen (for example, note the 60, 51 and 44 peaks in fig. 8). Thus, it can be seen in fig. 8 and figs. 9-12 that the PS depends upon the distribution of α as well as the width of the wave, i.e., upon σ_o. For instance in fig. 9 the weight in the peak corresponding to 44 msec., which is the result of the α-distribution shown, is greater than that in the peak at 33 msec., which was the value of t_p. The sharper the α-distribution the lower, in general, the level of the background in the PS (for example, compare these factors in figs. 9, 10, 11).

The most obvious deficiency in the PS in fig. 8 is the absence of a prominent 100 msec. peak. To compensate for this a "fine structure" was superimposed on the Poisson-like distribution of α. This fine structure usually consisted of grouping 3 successive values of α so that their values were set at 1.20, 0.90, 0.80, 1.20, 0.90, 0.80, 1.20, etc. times the corresponding values of the underlying Poisson-like distribution. Such a grouping was intended to produce a large 100 msec. effect (actually 99 msec. since it was not possible to specify t_p in units less than 1 msec.). The values of 1.20, 0.90, 0.80 were obtained from an examination of the height of the modes in the human data and gave better results than a large number of other triple values tested.

Two moderately successful attempts to duplicate the plot in fig. 6 are shown in figs. 10A and 11A. Plot 10A was obtained by normalizing the sum of the PS obtained from three separate runs (plots 10C-E). A number of obvious discrepancies still remain - such as high background, too large

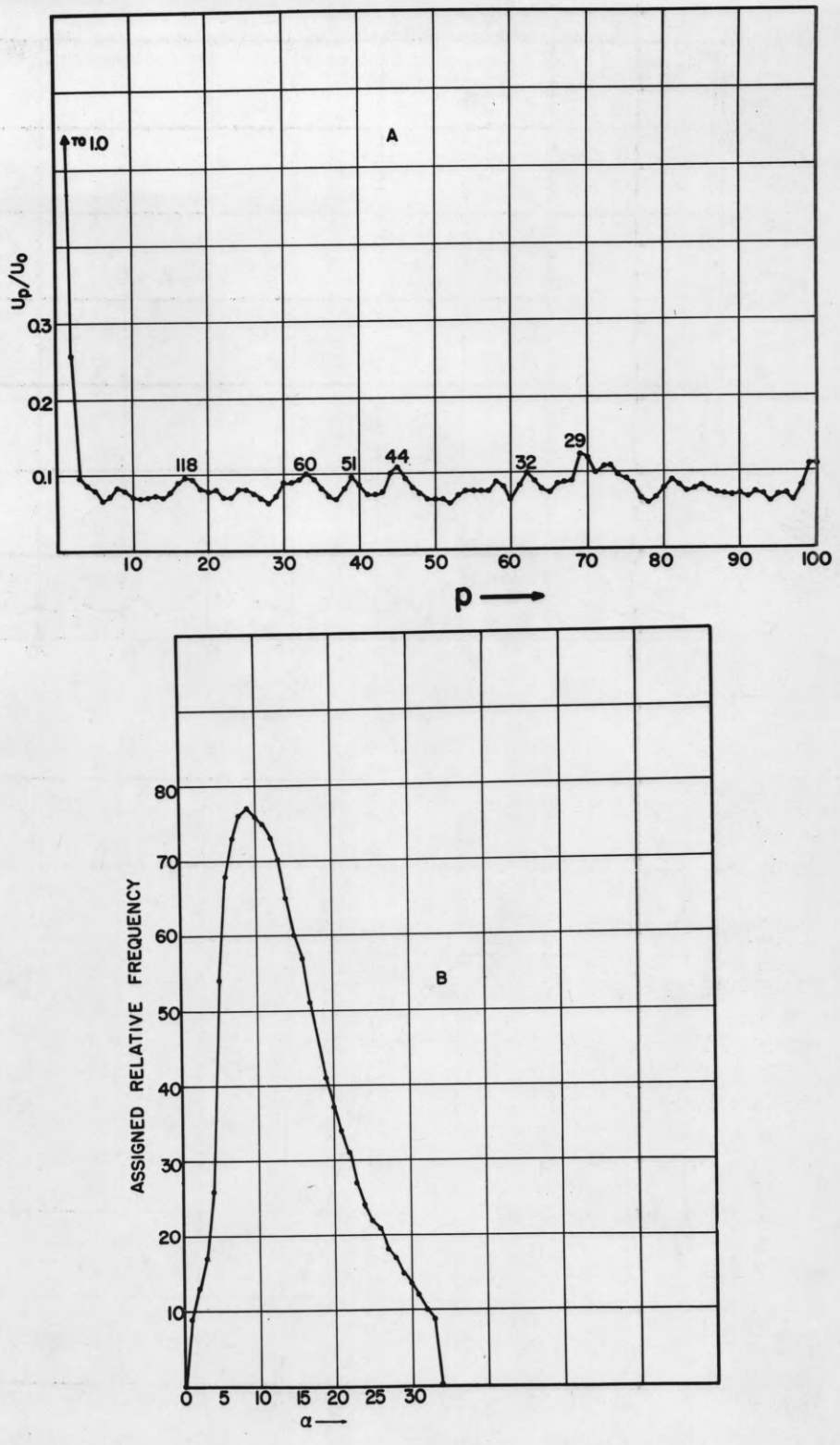

FIG. 8 PLOT A IS THE NORMALIZED SUM OF THREE PS GENERATED ACCORDING TO MIV USING THE FREQUENCY DISTRIBUTION OF α SHOWN IN PLOT B, t_p=100 msec., σ_o=30 msec., $1 \leq \alpha \leq 33$ AND S=400, EQUATION (1) HAD THE FORM:

$$T(\text{msec.}) = 400 + \Delta_o + 100\,\alpha$$

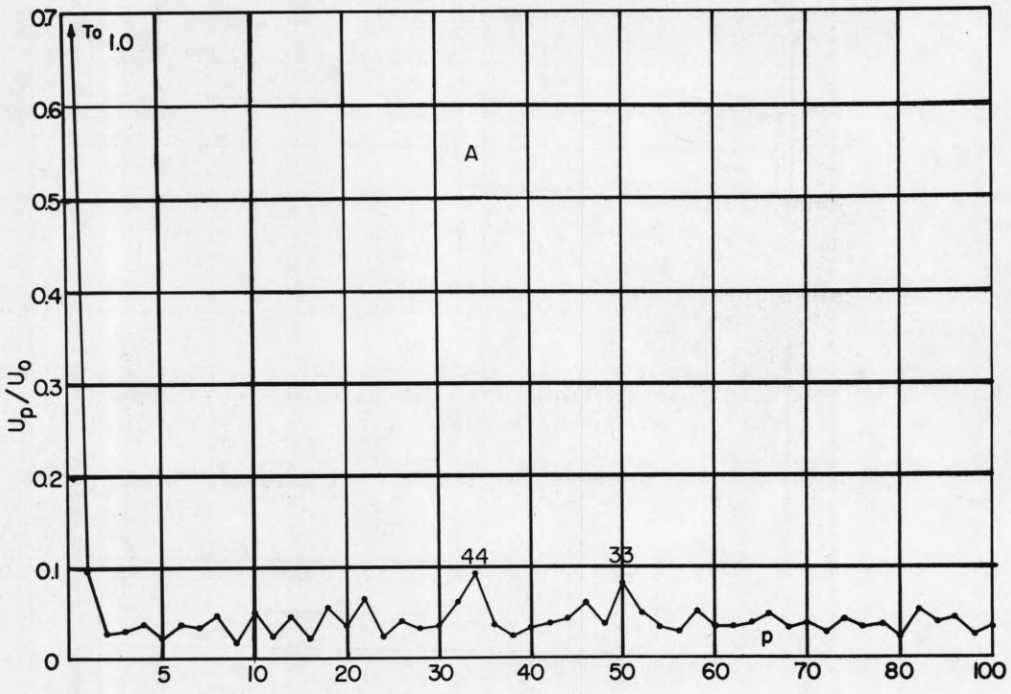

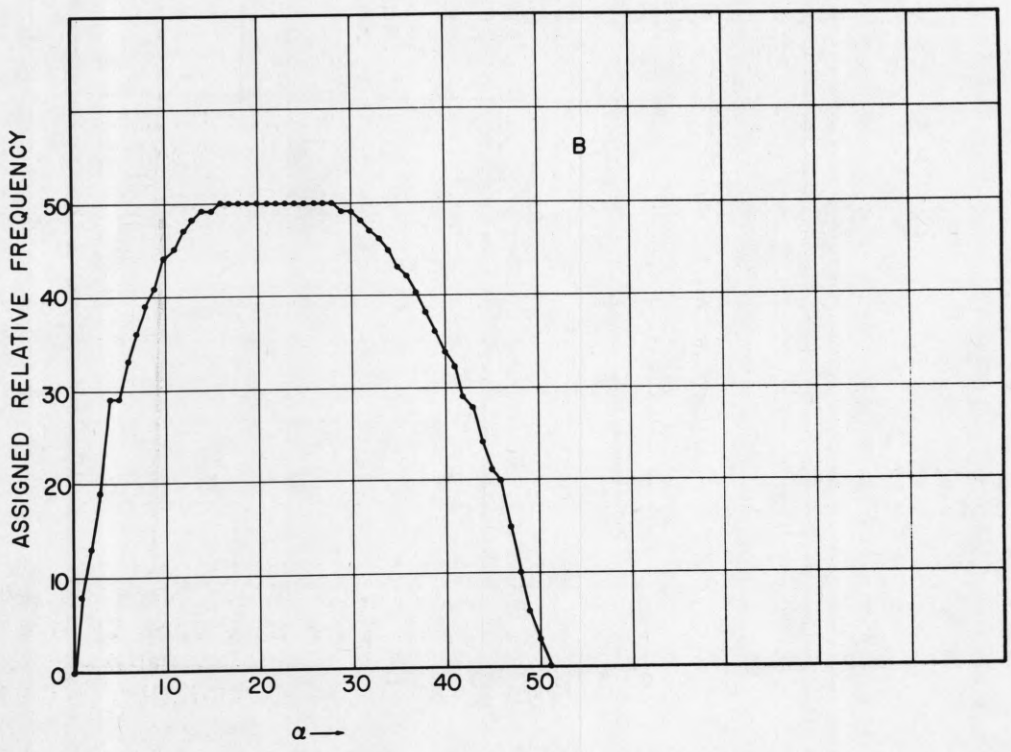

FIG. 9 PLOT A IS A PS GENERATED ACCORDING TO MIV USING THE FREQUENCY DISTRIBUTION OF α SHOWN IN PLOT B, t_p=33msec., σ_0=13msec., $1 \leq \alpha \leq 50$ AND S=200. WITH THESE FACTORS EQUATION (1) HAD THE FORM:

$$T(\text{msec.}) = 400 + \Delta_0 + 33\alpha$$

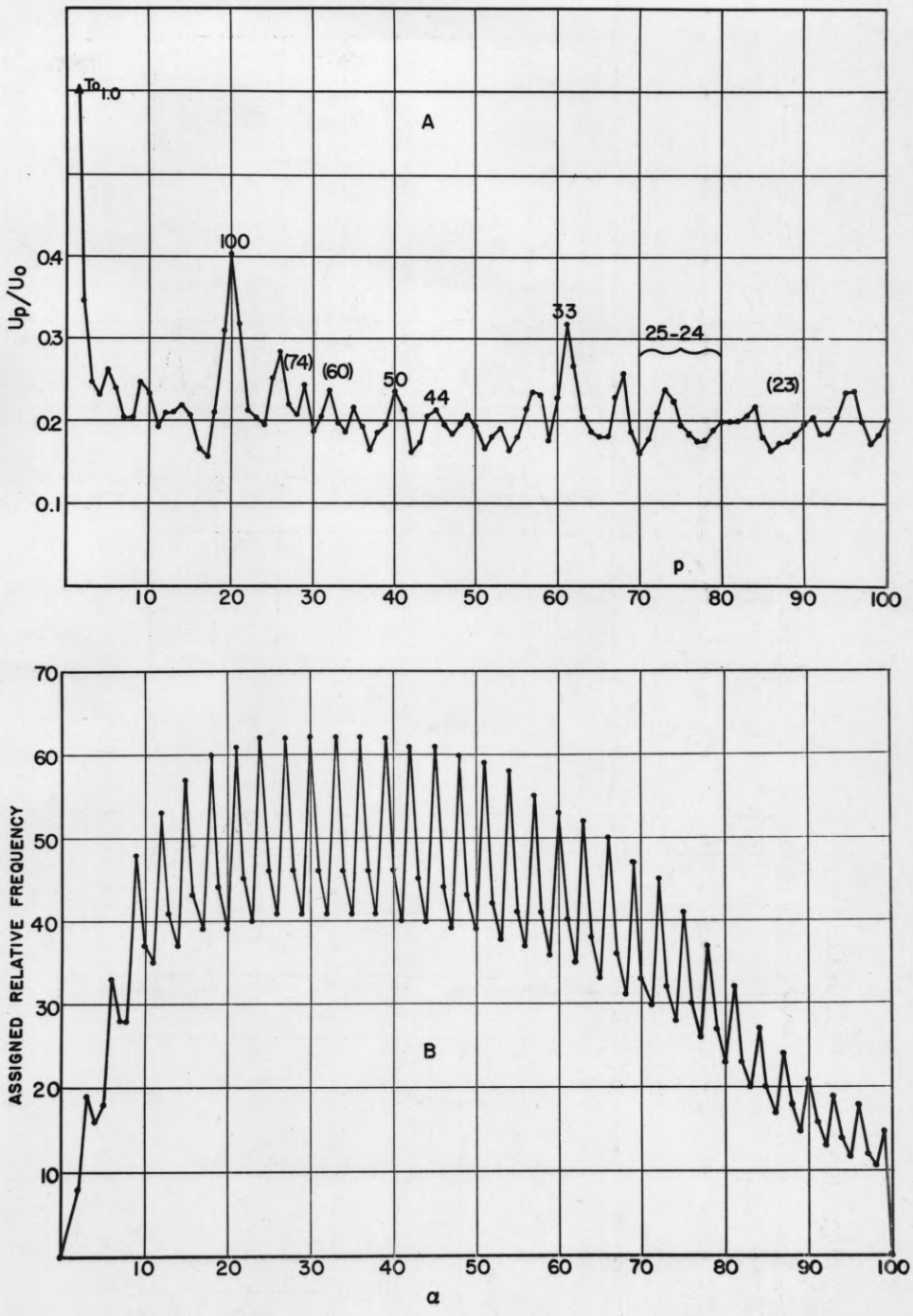

FIG. 10 PLOT A IS THE NORMALIZED SUM OF THE THREE PS SHOWN IN PLOTS C-E. THEY WERE GENERATED ACCORDING TO MIV USING THE FREQUENCY DISTRIBUTION OF α SHOWN IN PLOT B, $t_p = 33$ MSEC., $1 \leq \alpha \leq 100$ AND S=400. WITH THESE FACTORS EQUATION (1) HAD THE FORM:

$$T(\text{msec.}) = 400 + \Delta_0 + 33\alpha$$

THE POSITIONS OF THE PEAKS OBSERVED IN FIG. 6 ARE LABELED - THOSE IN PARENTHESES INDICATE PEAKS NOT OCCURING IN THIS PLOT.

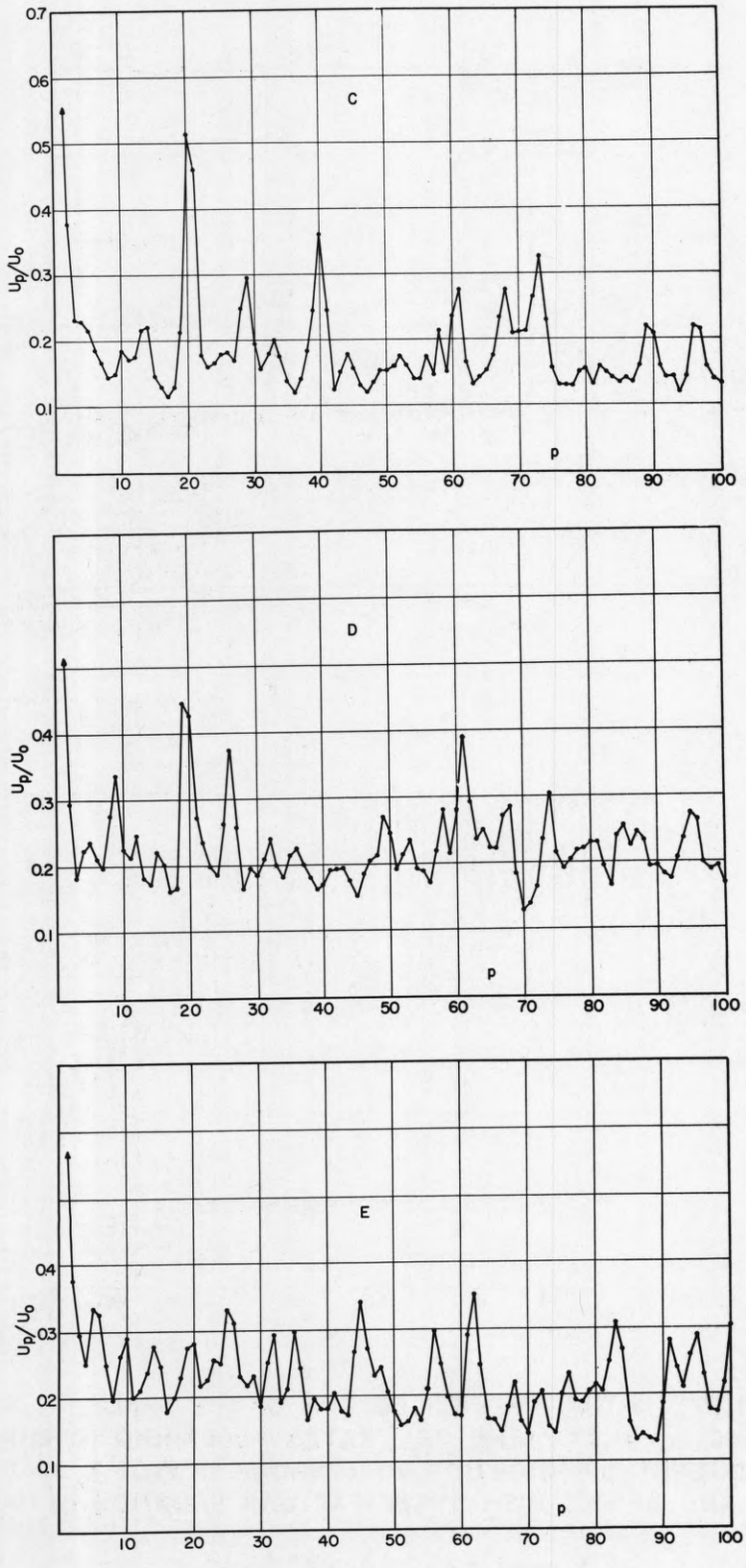

FIG. 10 (CONT'D)

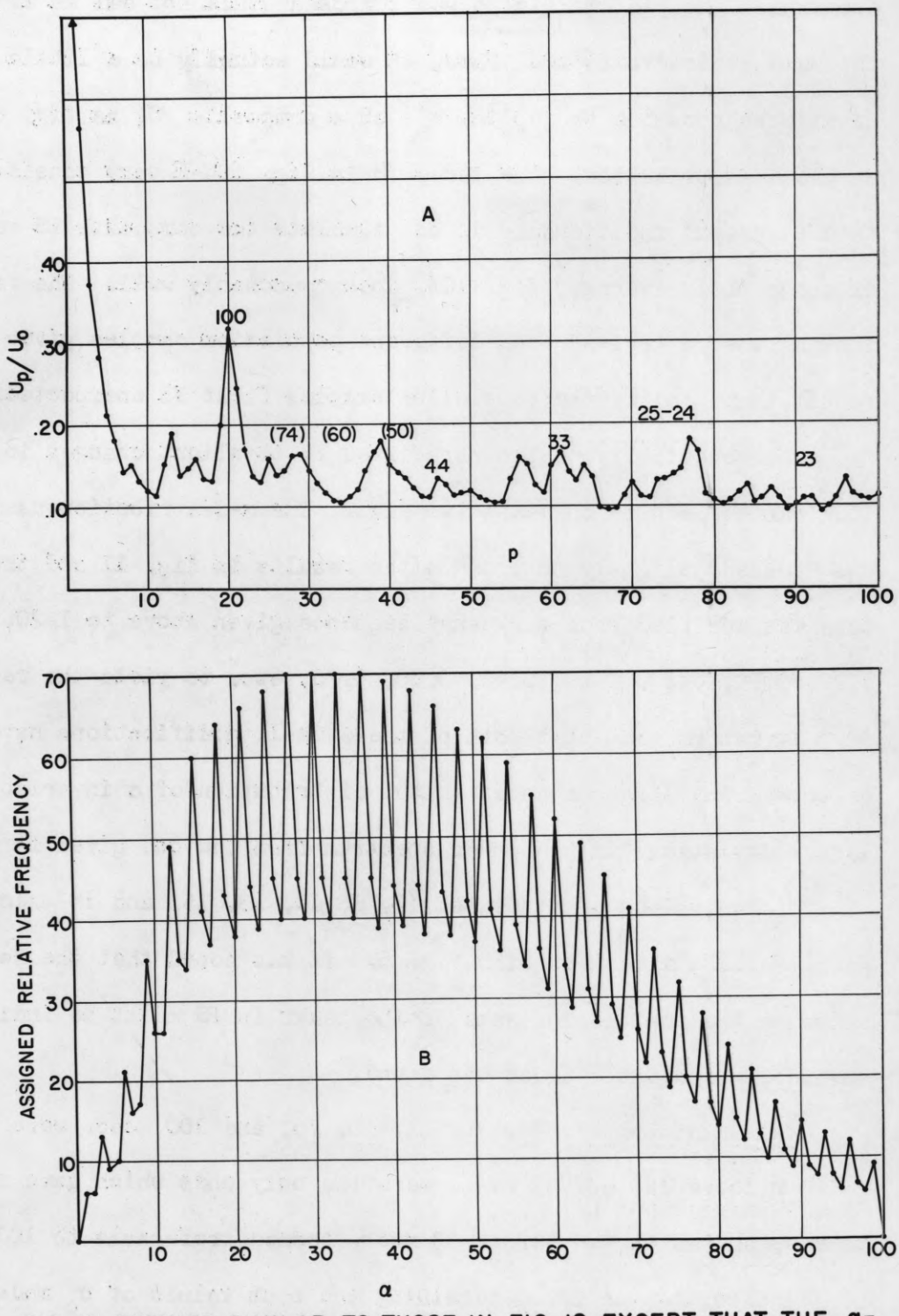

FIG. II RESULTS SIMILAR TO THOSE IN FIG. 10 EXCEPT THAT THE α-DISTRIBUTION IS SLIGHTLY MORE "PEAKED" THAN IN THE PREVIOUS RESULTS.

a 33 msec. peak, 50 and 44 msec. peaks too small, etc. However, the 21 PS from which the plot in fig. 6 was composed would not all be expected to have the same α-distributions. Thus, it would actually be a little surprising if it were possible to duplicate such a composite PS, as fig. 6, using a single α-distribution. The three PS in fig. 10C-E vary considerably among themselves and individually do not simulate the composite PS very closely, although their average, fig. 10A, does reasonably well. The fact that pooling the PS derived from different population samples gives a more stable result than pooling the population samples first is unexpected.

The sensitivity of the normalized PS to slight changes in the α-distribution can be seen in the last two figs. The α-distribution used in fig. 10 was "peaked" slightly to produce the results in fig. 11 and the fine structure was modified from the usual sequence given above to 1.20, 0.90, 0.80, 1.20, 0.90, 0.80, 1.20, 0.90, 0.80, 0.75, etc. to yield the results in fig. 12. It can be seen that both of these small modifications have significant effects. Any larger changes in the distribution of α invariably produced larger deviations in the power spectrum from the one given in fig. 6.

Of the values of σ_o tested (6, 8, 10, 13, 15, and 18 msec.) 13 msec. gave the best agreement with fig. 6. It was hoped that the height, the shape or the position of some of the peaks in PS might be indicative of σ_o. However, no reliable index was found.

Values of 25, 27, 33, 36, 44, 50, 75, and 100 msec. were assigned to t_p. Of these 100 and 33 msec. were the only ones which gave reasonable values, and as stated before 33 msec. seemed preferable to 100. The absence of a good criterion for determining the best values of σ_o made the task of determining appropriate values of the four parameters more difficult.

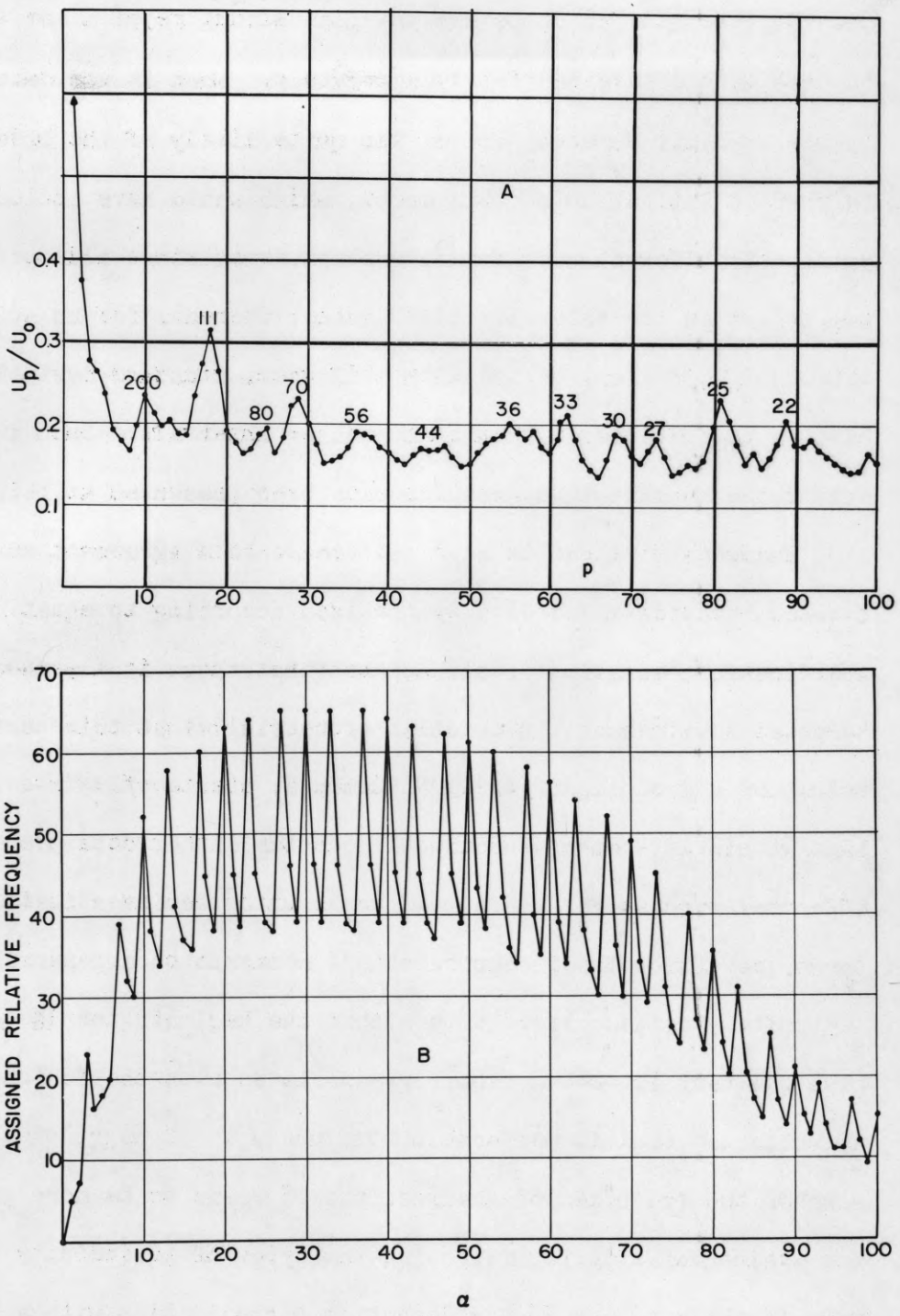

FIG. 12 PLOT A IS THE NORMALIZED SUM OF FIVE PS GENERATED ACCORDING TO MIV USING THE α-DISTRIBUTION SHOWN IN PLOT B, t_p=33 MSEC., σ_p=13 MSEC., $1 \leq \alpha \leq 100$ AND S=400. THE "FINE STRUCTURE" OF THE α-DISTRIBUTION GROUPED 3,3 AND 4 SUCCESSIVE VALUES TOGETHER RATHER THAN EVERY 3 AS IN THE PREVIOUS RESULTS (SEE TEXT FOR FURTHER EXPLANATION). NOTE THE RESULTING 111 MSEC. PEAK WHICH REPLACES THE USUAL 100 MSEC. ONE, AND ITS 56 MSEC. HARMONIC.

However, the general shape and the fine structure of α and the values of t_p have been determined fairly accurately. When it was determined that t_p was probably 33 msec. and σ_o was quite likely of the order of 13 msec., further investigation of this model, which would have included the investigation of different wave forms, was abandoned since all our human data were collected for intervals of 10 msec.; whereas, for an accurate investigation of a 33 msec. period with a 13 msec. standard deviation, data would have to be collected within much smaller intervals. Such a program is not envisioned so that these results have been presented at this time.

In summary it can be said that reasonable agreement can be obtained between human data and data synthesized according to equation 3, or its modification, equation 5. It appears that there is a period of 100 msec. associated with human information processing; that this period may be the result of a grouping of three fundamental quanta of 33 msec. duration; and that within a 33 msec. fundamental quantum either data processing or data input may occur. For the simple tasks which we investigated, t_o was of the order of 400 msec. Further there seems to be a general uncertainty, designated γ_o, associated with either the beginning or the cessation of a task but very little variability associated with the fundamental quanta by which the task is performed.

Of the two types of analyses the PS seems to be more sensitive than the autocorrelation for detecting the types of periodicity studied. The main drawback to the PS for detecting periodicities with a fairly disperse wave form is that the background is relatively high. The PS was found to be dependent upon the wave form, the duration of the periodicity, and the general shape of the time series (what we have referred to as the distribution of α in this paper).

Our mathematical model with the parameters used is compatible with the experimental findings from humans; however, this agreement does not exclude the possibility of other interpretations.

REFERENCES

1. Augenstine, L. G., in Information Theory in Psychology, Free Press, Glencoe, Illinois, Quastler (editor), p. 208-226 (1955).

2. Augenstine, L. G., "Human Performance in Information Transmission, Part VI: Evidence of Periodicity", Control Systems Laboratory, Urbana, Illinois, Report Number R-75, (1957).

3. Seiwell, H. R., Reviews of Sci. Instruments, 21: 481-484 (1950).

4. Tukey, J. W., "The Sampling Theory of Power Spectrum Estimates," Symposium on Applications of Autocorrelation Analysis to Physical Problems, Woods Hole, Massachusetts, 13-14 June 1949. ONR Publication NAVEXOS-P-735.

5. Tukey, J. W., "Measuring Noise Color," Bell Telephone Laboratories, publication prepared for distribution at a meeting of the Metropolitan Section, I. R. E., November 7, 1951.

6. Tukey, J. W., personal communication, (1953).

7. Abelson, R. P., "Spectral Analysis and the Study of Individual Differences in the Performance of Routine, Repetitive Tasks," Ph. D. Thesis, Princeton University, (1953).

8. Ross, D. T., "Improved Computational Techniques for Fourier Transformation", Servomechanisms Laboratory, Massachusetts Institute of Technology, Report Number 7138-R-5, (1954).

9. Churchill, R. V., Fourier Series and Boundary Value Problems, McGraw-Hill, Chaps. 5 and 6, (1941).

10. Margenau, H., and Murphy, G. M., The Mathematics of Physics and Chemistry, D. van Nostrand Co., Chap. 7, (1943).

APPENDIX

The following is a brief explanation of the significance of individual values of the autocorrelation function, R_k, and the spectral density function, U_p. For illustrative purposes, a hypothetical histogram is used with N = 31 points specified. All of the functions used in the Appendix are defined only at a number of discrete points. These points are connected with smooth curves only to aid in visualizing the general shapes of the functions, and not to represent intermediate values of the functions.

R_k (Equation 1) The kth autocorrelation term is the result of the following operations:

(i) displacement of the original histogram, x_i (Fig. 13A) k intervals to the left along the abscissa so as to form a second histogram, x_{i+k}, (Fig. 13B);

(ii) comparison of the two histograms point-by-point by forming the products $x_i \cdot x_{i+k}$ for i = 0, 1, 2 .... N-k (Fig. 13C);

and

(iii) forming the algebraic average, $\overline{x_i \cdot x_{i+k}}$, of the N-k products. The $\overline{x_i \cdot x_{i+k}}$ (which is the usual convariance for two functions) is a measure of how nearly identical the two histograms are. For example, if the histograms are practically identical for a lag of k, then most of the $x_i \cdot x_{i+k}$ terms would be positive and $\overline{x_i \cdot x_{i+k}}$ would be a large, positive value, whereas if the histograms are dissimilar the algebraic average would be close to zero. For zero lag (i.e., k = 0) $\overline{x_i \cdot x_{i+k}} = \overline{x_i^2}$ which, of course, is the maximum value this factor can assume. In the case of an absolutely periodic function, such as a sin or cos curve, the maximum value for $\overline{x_i \cdot x_{i+k}}$ would occur each time the lag was equal to an integral multiple of the period of the function, and the negative maximum would occur each time the lag was 1/2, 3/2, 5/2, etc. of the period.

Since the average amplitude is not constant in the experimental histograms, the mean and variance for the set of x_i's and the set of x_{i+k}'s will not necessarily be the same. In order to compensate for these two factors, the $\overline{x_i \cdot x_{i+k}}$ term has been modified as shown in Eq. 1. The modification chosen, in addition to helping correct for the variable mean and variance, is particularly convenient to use with automatic computation methods. Since $R_o = 1$, all R_k values are automatically normalized and in the proper form for plotting on the cathode ray tube.

To summarize: R_k is a measure of how near the histogram, x_i, is to being absolutely periodic for a lag of k (where a value of $R_k = 1$ would indicate complete periodicity with a period of k intervals). U_p (Equation 2). Using Fourier series, a function, f(x), can be represented in the interval $0 \leq x \leq L$ as the sum of a number of cosine components (9,10) of the form

$$(6)\quad f(x) \quad A_o + A_1 \cos \frac{\pi x}{L} + A_2 \cos 2 \frac{\pi x}{L} + \cdots + A_j \cos j \frac{\pi x}{L}$$

where the A_j terms are weighting factors which describe the relative importance of the corresponding cosine term of frequency j in representing f(x). The weighting terms, A_j, are of the form

$$(7)\quad A_j = \text{const} \sum_{x=o}^{L} f(x) \cos j \frac{x}{L}.$$

The analogies between equations (2), (6) and (7) are obvious ($U_p = A_j$, $R_k = f(x)$, $\frac{k\pi}{m} = \frac{x\pi}{L}$, and $p = j$). If the histogram, x_i, is periodic, R_k will have periodically large values corresponding to the periods in x_i, and thus its structure can readily be accounted for as the sum of a number of component frequencies. The pth spectral density term is the result of:

(i) comparing the autocorrelation values, R_k, (Fig. 13D) and the values of cos k p π/m (Fig. 13E) point-by-point by forming the products (R_k) (cos k p π/m) for k = 0, 1, 2, 3 .... m (Fig. 13F);

and

(ii) forming the sum of the m+1 products, (R_k) (cos k p π/m).

The sum, $\sum_k R_k$ cos k p π/m, which is the pth coefficient of the Fourier cosine series, is a measure of the importance of a cosine of frequency p in representing R_k. Thus the U_p values indicate the relative importance (or weight, or amplitude) associated with the component frequencies. As p is varied the relative importance of the component frequencies within the desired range can be determined.

As an aid in visualizing these analytical steps, the analysis is shown step-by-step for the 31-point histogram in Fig. 13. The detailed analysis is shown for k = 13 and p = 4. The complete set of values for the spectral density (Fig. 13G) function are also shown.

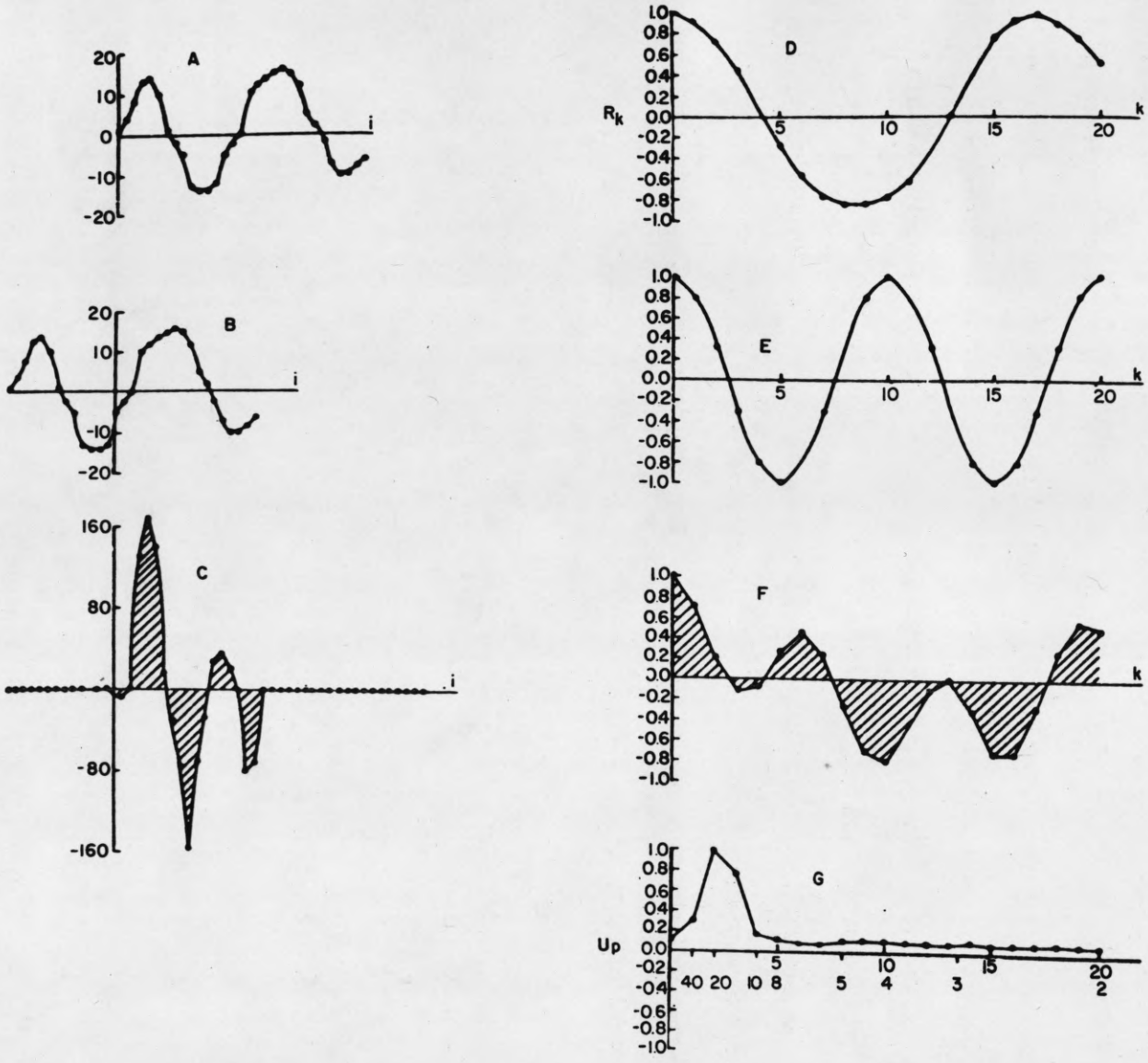
A
20
10
0
-10
-20
i
B
20
10
-10
-20
i
C
160
80
-80
-160
i
D
R_k
1.0
0.8
0.6
0.4
0.2
0.0
-0.2
-0.4
-0.6
-0.8
-1.0
5
10
15
20
k
E
1.0
0.8
0.6
0.4
0.2
0.0
-0.2
-0.4
-0.6
-0.8
-1.0
5
10
15
20
k
F
1.0
0.8
0.6
0.4
0.2
0.0
-0.2
-0.4
-0.6
-0.8
-1.0
k
G
Up
1.0
0.8
0.6
0.4
0.2
0.0
-0.2
-0.4
-0.6
-0.8
-1.0
40 20 10 8
5
5
4
10
3
15
20
2

FIG. 13

AUTHORIZED DISTRIBUTION LIST

As of March 18, 1958

Number of Copies	Agency
	Director of Research and Development Headquarters United States Air Force Washington 25, D. C.
1	Attn: AFDRD-AC/2
1	AFDRD-CC/2
	Commander Headquarters, Air Research and Development Command P. O. Box 1395 Baltimore 3, Maryland
1	Attn: RDDDR-5
	Headquarters, Air Force Office of Scientific Research Air Research and Development Command United States Air Force Washington 25, D. C.
1	Attn: SROP
	Commander Air Force Cambridge Research Center Laurence G. Hanscom Field Bedford, Massachusetts
1	Attn: CRR
	Commander Wright Air Development Center Wright-Patterson Air Force Base, Ohio
2	Attn: WCOSI-3
1	WCLG
1	WCRR
1	WCLR
1	WCLOT-2 (Mr. Cooper)
1	WCLRW (Mr. Overholt)
1	WCLRW (Mr. Clute)
	Commander USAF Security Service San Antonio, Texas
1	Attn: CLR
	Commanding Officer Rome Air Development Center
1	Griffiss Air Force Base, New York

Number of Copies	Agency	
	Director Air University Library Maxwell Air Force Base, Alabama	
1	Attn: CR-4803a	
	Commander Air Force Armament Center Eglin Air Force Base, Florida	
1	Attn: Deputy for Operations	
	Chief, Bureau of Ships Department of the Navy Washington 25, D. C.	
2	Attn: Code 280	Code 820 (1)
1	Code 565C	Code 825 (1)
1	Code 810	Code 830 (1)
1	Code 810B	Code 835 (1)
1	Code 812	
	Chief, Bureau of Aeronautics Department of the Navy Washington 25, D. C.	
1	Attn: EL-402	
1	TD-4	
	Department of the Navy Office of Naval Research Washington 25, D. C.	
1	Attn: Code 900	
1	Code 430	
2	Code 437	
	Commanding Officer Office of Naval Research Chicago Branch John Crerar Library Building 10th Floor, 86 E. Randolph St.	
1	Chicago 1, Illinois	
	Bureau of Ordnance Department of the Navy Washington 25, D. C.	
1	Attn: Re4C	
	Director Office of Naval Research Branch Office 1000 Geary Street	
1	San Francisco, California	

Number of Copies	Agency
(Progress Reports Only)	U. S. Navy Inspector of Ordnance Applied Physics Laboratory The Johns Hopkins University 8621 Georgia Avenue
2	Silver Springs, Maryland
	Commanding Officer and Director U. S. Naval Electronics Laboratory San Diego 52, California
1	Attn: Library
1	Code 2800, C. S. Manning
	Director Naval Research Laboratory Washington 25, D. C.
1	Attn: Code 4100
1	Code 3620
1	Code 1100
	Chief of Naval Operations Navy Department Washington 25, D. C.
1	Attn: OP-51
1	OP-371-C
1	OP-551
1	OP-341-D
	Commanding Officer Naval Air Development Center Johnsville, Pennsylvania
1	Attn: Code AAEL
	Commander Naval Ordnance Laboratory White Oaks Silver Springs 19, Maryland
1	Attn: Technical Library
	Head, Combat Direction Systems Branch (OP-345) Department of the Navy Room 4C-518 Pentagon
1	Washington 25, D. C.
	Department of the Army Office of the Chief Signal Officer Washington 25, D. C.
1	Attn: SIGRD
1	SIGRD-9-b

Number of Copies	Agency
1	Chief of Research and Development Office of the Chief of Staff Department of the Army Washington 25, D. C.
1	Asst. Chief of Staff, Development and Test Headquarters, Continental Army Command Fort Monroe, Virginia
1	President, U. S. Army Airborne and Electronics Board Continental Army Command Fort Bragg, North Carolina
1	President, U. S. Army Defense Board Continental Army Command Fort Bliss, Texas
1 1	Office of the Chief of Ordnance Department of Ordnance Washington 25, D. C. Attn: ORDTR ORDTB
1	Commanding Officer Office of Ordnance Research 2127 Myrtle Drive Duke Station Durham, North Carolina
3	Director Ballistics Research Laboratory Aberdeen Proving Ground, Maryland Attn: Dr. L. A. Delsasso
1	Commanding Officer Frankford Arsenal Philadelphia 37, Pennsylvania
2	Commanding General Redstone Arsenal Huntsville, Alabama Attn: Technical Library
1	9560 S. C. Electronics Research Unit P. O. Box 205 Mountain View, California

Number of Copies	Agency
20	Transportation Officer Fort Monmouth Little Silver, New Jersey Marked For: SCEL Accountable Property Officer Bldg. 2700 Camp Wood Area Inspect at Destination File No. 0060-PH-54-91 (5308)
1	Director National Bureau of Standards Washington 25, D. C. Attn: Dr. S. N. Alexander
1	Librarian Instrumentation Laboratory Massachusetts Institute of Technology Cambridge 39, Massachusetts
1	Director Jet Propulsion Laboratory California Institute of Technology Pasadena, California
1	Chicago Midway Labs 6040 South Greenwood Avenue Chicago 37, Illinois Attn: Librarian
1	Hughes Research and Development Library Hughes Aircraft Company Culver City, California Attn: Miss Mary Jo Case
1	Mr. Robert R. Everett Division Head Lincoln Laboratory Massachusetts Institute of Technology Lexington 73, Massachusetts
1	Technical Documents Service Willow Run Laboratories University of Michigan Willow Run Airport Ypsilanti, Michigan
6	Armed Services Technical Information Agency Arlington Hall Station Arlington 12, Virginia

Number of Copies	Agency
	The RAND Corporation 1700 Main Street Santa Monica, California
1	Attn: Library
	Dr. C. C. Furnas Cornell Aeronautical Laboratory
1	Buffalo, New York
	Massachusetts Institute of Technology Lincoln Laboratory P. O. Box 73
1	Lexington 73, Massachusetts
	W. L. Maxson Corporation 460 West 34th Street
1	New York 1, New York
	Stanford University Electronics Research Laboratory
1	Stanford, California
	Radio Corporation of America RCA Laboratories Division David Sarnoff Research Center Princeton, New Jersey
1	Attn: Mr. A. W. Vance
	The Johns Hopkins University Operations Research Office 6410 Connecticut Avenue Chevy Chase, Maryland
1	For: Contract DA 44-109-qm-266
	Light Military Electronic Equipment Department General Electric Company French Road Utica, New York
1	For: Contract AF 33 (600)-16934
	Goodyear Aircraft Corporation Akron 15, Ohio
1	For: Project MX 778 Contract W33-039 ac-14153
	Mr. A. A. Lundstrom Bell Telephone Laboratories
1	Whippany, New Jersey

Number of Copies	Agency
	Litton Industries 336 North Foothill Road Beverly Hills, California via: Inspector of Naval Materiel
1	Los Angeles, California
	Remington Rand Univac Division of Sperry Rand Corporation via: Insmat, BuShips Insp. Officer 1902 West Minnehaha Avenue
1	St Paul 4, Minnesota
	Technical Library Code 142 David Taylor Model Basin
1	Washington 7, D. C.
	Commanding Officer and Director David Taylor Model Basin Washington 7, D. C.
1	Attn: Code 800
	Naval Ordnance Proving Ground Computation Center Dahlgren, Virginia
1	Attn: R. A. Niemann
	System Development Corporation 2500 Colorado Avenue
1	Santa Monica, California